J. Membrane Biol. 132, 41–52 (1993)

The Journal of
Membrane Biology

A Nonlinear Filter Algorithm for the Detection of Jumps in Patch-Clamp Data

Roland Schultze and Silke Draber
Institut für Angewandte Physik der Universität Kiel, DW-2300 Kiel 1, Germany

Summary. This paper presents a new algorithm for the detection of channel openings and closures from noisy current signals, especially for the correct generation and interpretation of open-time and closed-time histograms. The Hinkley detector is a nonlinear off-line jump detection algorithm from the field of fault detection. Here, an improved version, the higher-order Hinkley detector H.O.H.D., is developed. A general description of the sensitivity of a detector is introduced by the time resolution t_{res}. This allows a comparison of the nonlinear detectors with the standard threshold detectors preceded by a low-pass filter for noise suppression. By means of application to simulated and real data, the performance of the detection algorithms is investigated. The higher-order Hinkley detector gave the best results with respect to correct reconstruction of the event length, to a small amount of missed brief events as well as to the ability to achieve short time resolution without pretending false events, especially in the presence of colored noise.

Key Words patch clamp · fault detection · jump detection · dwell-time histograms

Introduction

The patch-clamp technique (Sakmann & Neher, 1983; Hedrich & Schroeder, 1989) is of great importance for the investigation of transport through biological membranes. It provides the facility of measuring the current through a single channel protein and of investigating the dependence of current and gating dynamics on membrane voltage and on the concentrations of ions and various agents.

There are three, structurally different methods of analyzing channel openings and closures.

(1) The **direct way** is a jump-detection algorithm, normally a Bessel filter with subsequent threshold detection. It results in open-time and closed-time histograms. Until now this technique was restricted to events longer than about 100 μsec.

(2) For the time scale of 10 to 100 μsec the analysis of **beta functions** (FitzHugh, 1983) was applied (Yellen, 1984; Klieber, 1990). Short undetected closures (gaps) can be recognized as they distort the open channel amplitude histogram which is no longer a Gaussian distribution, but an asymmetric beta function.

(3) With even faster events, the beta functions become again very similar to Gaussian amplitude distributions. Now, the information about fast switching can be gained only from a comparison of the noise of the open and the closed level. Analysis based on this effect is known as investigation of the **open channel excess noise** (Heinemann & Sigworth, 1988).

Although methods (2) and (3) are applicable to fast-blocking kinetics, the direct method (1) is preferable, whenever possible. The results are several time constants and amplitude factors of the exponentials, evaluated from the dwell-time histograms. Thus, they comprise more information than the two parameters of a beta function or just the variance of the excess noise. In the following we deal with the problem of extending the temporal resolution of the direct method (1).

Fig. 1*A* shows a typical low-noise time series of pipette current measured with our fast setup at a sampling frequency of 100 kHz. The slow switching between four levels of current indicates that at least three channels are within the patch. Besides this slow switching, short gaps of about 30 μsec duration and some short openings can be recognized. This paper shows how to reach the aim of resolving these fast gating processes by the direct method (1).

For the construction of dwell-time histograms, algorithms are required for the correct identification of open times and closed times in the presence of inevitable background noise. The problem can be described as follows: A signal jumps between two or more equally spaced levels which are constant and known a priori. But the signal is corrupted by additional noise, which may roughly be considered as Gaussian white noise. From this noisy signal the original jumps are to be detected.

In the field of technical signal analysis and fault detection, many engineers and statisticians are concerned with similar problems (Basseville, 1986). For the problem characterized above, the appropriate solution is the Hinkley detector (Page, 1954,

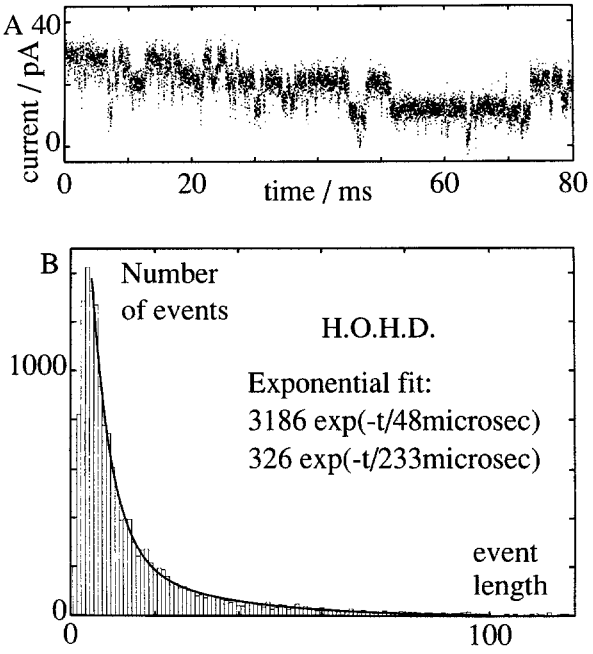

Fig. 1. (*A*) Time series (8,000 samples) of real patch-clamp data from tonoplast vesicles of *Chara*. Original raw data, prefiltered with an antialiasing Bessel filter with a cutoff frequency (−3dB) of 25 kHz and sampled at 100 kHz. Signal-to-noise ratio is about 4. (*B*) Closed-time histogram obtained with the H.O.H.D. from the whole record comprising 6,000,000 samples. The time axis of the event length contains bins 1 (10 μsec) to 120 (1.2 msec). The double-exponential fit reveals two time-constants: 48 μsec and 233 μsec.

1955; Hinkley, 1971), sometimes called likelihood ratio test or cumulative sum algorithm (Nikiforov, 1986). Basseville and Benveniste (1986) give a comprehensive review of methods for detection of changes in signals and systems.

By a combination of experimental noise reduction (excised patch, coated pipettes), fast sampling and nonlinear off-line detection by the higher-order Hinkley detector (H.O.H.D.), presented in this paper, we have extended the resolution of the direct approach (1) to 10–20 μsec. This opens the possibility to access the interesting gating phenomena in the range shorter than 100 μsec. It might be possible to resolve the blocked state of a calcium channel with a lifetime of 60 μsec, suggested by Pietrobon, Prod'hom and Hess (1988), and the fast gating processes involved in the blockage of the potassium channel by thallium (Draber, Schultze & Hansen, 1991), cesium (Klieber, 1990) or sodium (Bertl, 1989).

Four Alternative Methods for Reconstruction of Single Channel Events (Jump Detection)

Noise hinders the proper detection of jumps in the current of patch-clamp recordings. We compare four algorithms with respect to their ability to reconstruct the original channel signals from noisy records.

In the following calculations z_t ($t = 0, 1, 2, \ldots, N$) stands for the noisy raw data delivered by the patch-clamp amplifier or by the simulated model. The detection of an opening requires the determination of a transition of z_t from μ_0 (closed state) to μ_1 (open state). Without loss of generality we assume $\mu_1 > \mu_0$. Jumps to a lower level are treated in the same way but with inverted signs. As z_t is noisy, we cannot look at individual values of z_t, but have to use something like a weighted time average. Different averaging procedures are provided by the four filter algorithms described below.

All these algorithms possess a "turning knob" which influences the sensitivity (the thresholds λ or λ^8 for the nonlinear Hinkley detectors and the cut-off frequency f_{3dB} for the linear low-pass methods). A suitable parameter for the quantitative comparison of sensitivity is defined under the condition of no noise. The time resolution t_{res} of a detector, measured in units of sampling steps, is the length of the shortest event which is detected by the individual detector. The following subsections establish the connection between the specific "turning knob" of the detector and the general description of the sensitivity by means of the time resolution. It is possible to compare the behavior of the different types of detectors, after they are adjusted to have the same time resolution.

The Hinkley Detector

The operation of the Hinkley-detector algorithm is based on the construction of a series of test values g_t in the following way:

First, set $g_0 := 0$.

Now the time series z_t is scanned by recursively calculating the cumulative sum

$$g_t = g_{t-1} + \left(z_t - \frac{\mu_0 + \mu_1}{2}\right) \tag{1}$$

So far this is a linear operation on z_t. Nonlinearity is introduced by setting the g_t values calculated by Eq. (1) immediately to zero if they become negative

$$g_t = \max(g_t, 0) = \begin{cases} g_t & \text{if } g_t \geq 0 \\ 0 & \text{if } g_t < 0 \end{cases} \tag{2}$$

before applying Eq. (1) again.

The behavior of the test value g_t is depicted in Fig. 2. As long as the channel is closed, the mean

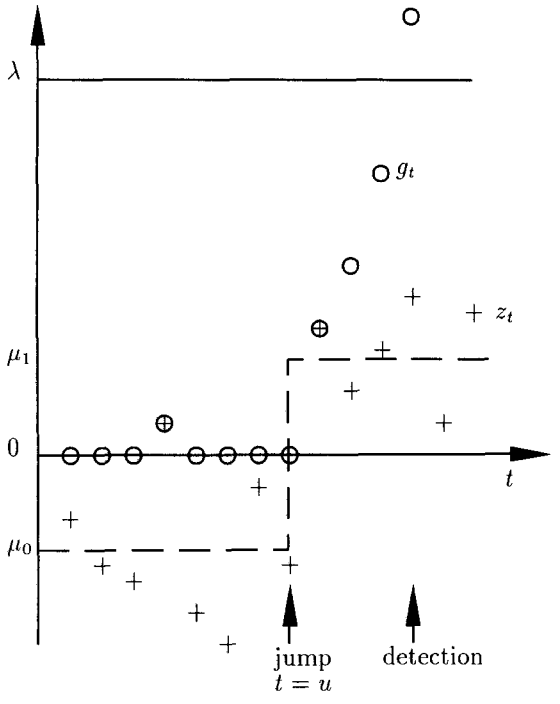

Fig. 2. Detection of a jump in the noisy time series z_t(+) by means of the test value series g_t (○) crossing the threshold λ. The broken line shows the mean value of z_t jumping from μ_0 to μ_1, but this signal is, of course, unknown to the detector. The choice $\mu_0 + \mu_1 = 0$ is not a prerequisite for the algorithm. (*modified from* Schultze, 1992)

value of z_t is μ_0. Insertion of $z_t = \mu_0$ in Eq. (1) shows that g_t decreases by being smaller than g_{t-1} ($\mu_1 > \mu_0$) and therefore reaches $g_t = 0$, where it remains stationary because of Eq. (2). Due to noise, however, it is possible that g rises for individual samples to positive values, if $z_t > (\mu_0 + \mu_1)/2$.

After the jump, when the channel has opened, say at time $t = u$, the mean value of z_t is μ_1. For the noise-free case $z_t = \mu_1$ the test value g starts to rise as

$$g_t = g_{t-1} + \left(\mu_1 - \frac{\mu_0 + \mu_1}{2}\right)$$

$$= g_{t-1} + \left(\frac{\mu_1 - \mu_0}{2}\right) \tag{3}$$

$$g_t = \frac{\mu_1 - \mu_0}{2} \cdot (t - u). \tag{4}$$

Figure 2 shows the test value g_t as circles. The broken line gives the ideal, undisturbed jump of z_t which the detector actually does not know. Before the jump occurs, the test value g_t is mostly zero and only sometimes obtains a small positive value. The change of the behavior of the test value after the jump is obvious: it definitely starts to grow (Eq. (4)). It is now intuitively clear how to exploit this behavior for an automated jump detection. Setting a threshold λ for the g_t values, allows us to distinguish the jumps of z_t from the effects of noise. After jump detection, the moment of the jump is determined by backward calculation. The known time course of the test value g_t provides a good means of estimating the exact moment of the jump. In Fig. 2 g_t equals zero directly before the jump occurs. It is therefore a natural way to estimate the jump moment to be the last moment before the jump detection with $g_j = 0$. This possibility of estimating a time $t = j$ of the jump which lies before the detection is an advantage of the off-line application.

After jump detection the algorithm starts again with $g_j := 0$ at time j with inverse signs, as now a jump from μ_1 down to μ_0 is to be detected.

The threshold λ determines the sensitivity of the detector which can also be described in terms of the time resolution t_{res}, the general parameter of sensitivity. The relation between t_{res} and λ is obtained from the response of the detector to a noise-free opening of length t_{res}. Equation (4) states that a noise-free opening from u until $u + t_{res}$ lets the test value g_t grow up to

$$g_{u+t_{res}} = \frac{\mu_1 - \mu_0}{2} \cdot t_{res} \tag{5}$$

Setting λ to this value

$$\lambda = \frac{\mu_1 - \mu_0}{2} \cdot t_{res} \tag{6}$$

leaves all shorter events than t_{res} undetected and all longer events detected.

It has to be kept in mind that a shorter time resolution favors false detections. That means that a lower threshold λ can be exceeded more easily "by accident" even though no jump has occurred. A reliable adjustment of the sensitivity of the detector is discussed below in the section on False Alarms.

With more than one channel under examination the algorithm is not much more complicated. One has to look simultaneously for upward and downward jumps.

Higher-Order Hinkley Detector

In terms of the frequency domain, the detectors are used in order to cut off the high frequency noise. The Hinkley detector is based on the first-order dif-

ference equation (1). This leads to a weak attenuation of the higher frequencies with a f^{-1} slope.

As known from Bessel filters, the performance gets better if the order is increased, normally to eight. Thus, we developed the higher-order Hinkley detector. It differs from the Hinkley detector because it does not use the simple cumulative sum (first-order integral) of the signal but the eighth-order integral (or cumulative sum). The high frequency attenuation is much stronger, roughly with a f^{-8} slope. The benefit of this modification becomes clear in the section Example of Simulation and Detection. The upward and downward bending traces of the test values g_t^8 are smoother in the case of the H.O.H.D. than g_t of the standard HINKLEY detector. Equations (1) and (2) are replaced by the eighth-order cumulative sum calculated by the following equations

$$\begin{aligned} g_t^1 &= g_{t-1}^1 + \left(z_t - \frac{\mu_0 + \mu_1}{2}\right) \\ g_t^2 &= g_{t-1}^2 + g_t^1 \\ g_t^3 &= g_{t-1}^3 + g_t^2 \\ g_t^4 &= g_{t-1}^4 + g_t^3 \\ g_t^5 &= g_{t-1}^5 + g_t^4 \\ g_t^6 &= g_{t-1}^6 + g_t^5 \\ g_t^7 &= g_{t-1}^7 + g_t^6 \\ g_t^8 &= g_{t-1}^8 + g_t^7 \end{aligned} \tag{7}$$

and a synchronous cutting to zero

$$g_t^i = \begin{cases} g_t^i & \text{if } g_t^1 \geq 0 \\ 0 & \text{if } g_t^1 < 0 \end{cases}$$

$$(i = 1, 2, 3, \ldots, 8) \tag{8}$$

A jump is detected when the eighth-order cumulative sum g_t^8 crosses a threshold λ^8 which determines the sensitivity of the H.O.H.D. The jump moment j is obtained by backward estimation as in the case of the Hinkley detector described above. For a given time resolution t_{res}, the threshold λ^8 for g^8 has to be the maximum of the g^8 values occurring as response to a noise-free opening event of length t_{res} and amplitude $\mu_1 - \mu_0$.

We did not try other orders than eight because this seemed to us to be a good compromise between strong cutoff of high frequencies and acceptable computational complexity.

First-Order Low Pass with Threshold Detector

As mentioned in the introduction, the common method of noise suppression is low-pass filtering, mostly applied to analog data before sampling and storing. Afterwards, the detection of jumps is simply accomplished by half-amplitude threshold analysis (Colquhoun & Sigworth, 1983), observing the filtered signal exceeding the thresholds halfway between the mean levels.

The first-order filter used for the comparison with the Hinkley detectors is a digital low-pass filter because sampled data (simulated or real) are analyzed. As the threshold analysis works in the time domain, the digital low pass must have the same impulse-response as the analog low pass. Therefore, we applied the invariant impulse-response method (Antoniou, 1979) for the calculation of the digital low pass.

The mentioned "turning knob" for the adjustment of the sensitivity is the frequency f_{3dB} of 3dB attenuation. It is related to the time resolution t_{res} (the duration of a noise-free opening reaching the half-amplitude threshold) by the equation

$$f_{3dB} = f_s \cdot \frac{\ln(2)}{2\pi \cdot t_{res}} \approx f_s \cdot \frac{0.11}{t_{res}} \tag{9}$$

with f_s being the sampling frequency, and t_{res} given in units of sampling steps as usual.

As we show below, the low-pass method tends to produce many more "false alarms" than the Hinkley detector does. This bad performance of the first-order low pass can be avoided by using a higher-order filter.

Bessel Filter with Threshold Detector

As pointed out by Colquhoun & Sigworth (1983) the eight-pole Bessel filter is an approximation of the Gaussian filter. It is commonly used for jump detection because it exhibits a linear phase behavior in the passband and a very smooth step response. The price for this advantage is a soft transition between passband and cutoff in the frequency domain. This is a good deal for filtering of patch-clamp data because a linear phase response is necessary in order to conserve the pulse shape, whereas the frequency spectrum is of minor interest.

The relationship between the frequency f_{3dB} of 3dB attenuation and the time resolution t_{res} (which is the length of a square pulse reaching the threshold of half its original amplitude after filtering) is given by

$$f_{3dB} = f_s \cdot \frac{0.18}{t_{res}} \tag{10}$$

with the sampling frequency f_s and the time resolution t_{res} given in units of sampling intervals.

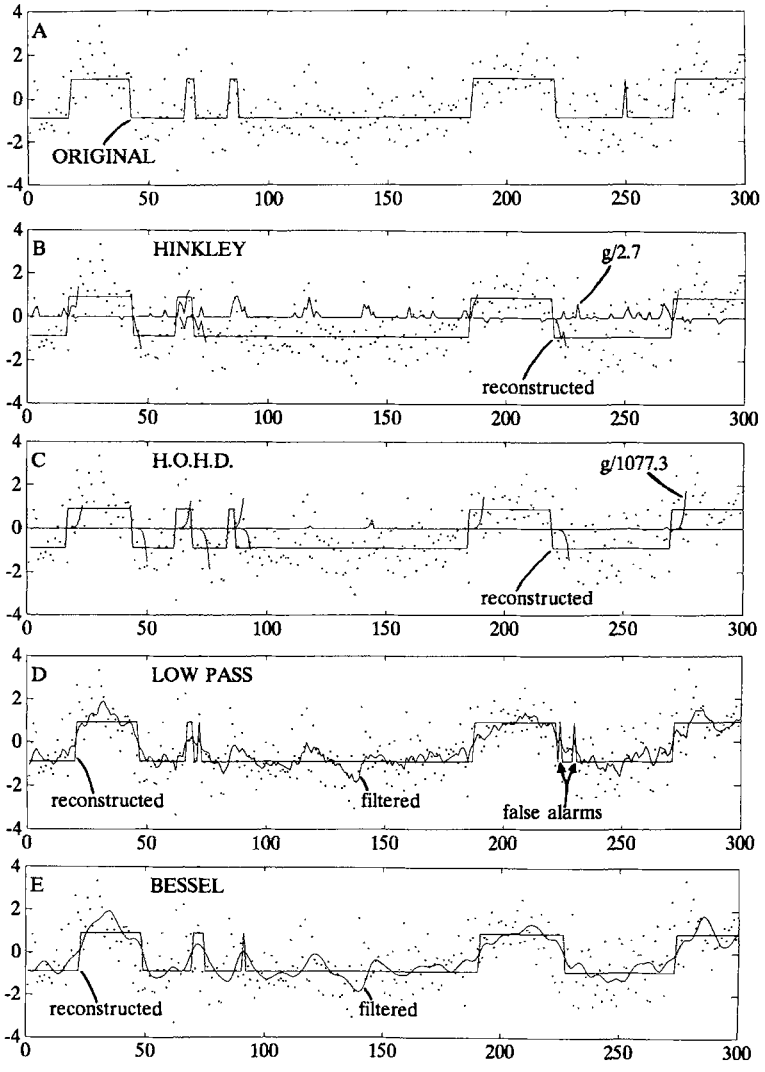

Fig. 3. Example of simulation and detection. Data are generated by random switching of a two-state model (Eq. (11)): $k_{oc} = 0.05$, $k_{co} = 0.03$, $\mu_0 = -0.9$, $\mu_1 = 0.9$. 300 samples with superimposed noise $\sigma = 1$ SNR = 1.8. Temporal resolution of the detectors $t_{res} = 3$. (*A*) ORIGINAL and noisy time series. The noisy time series (dots) is also given as background in traces *B*, *C*, *D*, *E*. (*B*) Time series reconstructed by the HINKLEY detector. Notice the missed event at sample 85. The short upward and downward bending traces are the series of test values g_t. For this plot we divided g_t by $\lambda = 2.7$. (*C*) Time series reconstructed by the higher-order Hinkley detector. The series of test values g_t^8/λ^8 is scaled with $\lambda^8 = 1077.3$. It is smoother than g_t/λ in *B*. (*D*) First-order LOW-PASS filtered time series. The signal is reconstructed by threshold analysis. Notice that the filtered signal crosses the threshold five times at sample 230, which produces four additional short events. (*E*) Time series reconstructed by BESSEL filter and threshold detection.

We use the Bessel filter coefficients proposed by Antoniou (1979) who also gives an example of the transformation of a Bessel filter by the invariant impulse-response method. The threshold analysis is performed in the same way as in the case of the first-order low pass.

Example of Simulation and Detection

For the following simple example we simulate the switching of a channel with one open and one closed state:

$$O \underset{k_{co}}{\overset{k_{oc}}{\rightleftharpoons}} C \tag{11}$$

The rate constants $k_{oc} = 0.05$, $k_{co} = 0.03$ refer to the transition probability per sampling interval.

The randomly switching channel is simulated by means of a random generator which decides about jumps from one state to another with a probability according to the rate constants k_{oc}, k_{co}. Assigning the levels μ_0, μ_1 of pipette current to the closed and the open state, respectively, results in a noise-free signal called "ORIGINAL" consisting of discrete jumps between these two levels. The solid line in Fig. 3*A* shows the ORIGINAL time series jumping between $\mu_0 = -0.9$ and $\mu_1 = 0.9$. The half-jump magnitude is $p = (\mu_1 - \mu_0)/2 = 0.9$. Addition of white Gaussian noise with standard deviation $\sigma = 1.0$ yields the noisy time series which is displayed as dots in Fig. 3*A*. The signal-to-noise ratio, defined as SNR $= 2p/\sigma$, is 1.8.

The simulated noisy data is fed into the detectors in order to reconstruct the original signal. The parameters of the four algorithms are adjusted to give the same time resolution.

The performance of the HINKLEY detector is demonstrated in Fig. 3*B*. The solid line switching

between two levels, gives the detected events. The noisy line flickering upward and downward around zero shows the behavior of the test value g_t/λ (Eqs. (1) and (2)). The scaled time series g_t/λ is displayed in order to use "1" as a reference for detection. Figure 3*B* shows that g_t goes upward until the upward jump is detected at sample 20. After the jump detection, the algorithm starts with inverted signs from the estimated jump moment. Therefore the g_t tails are now bent downward until a jump to the closed level μ_0 is detected at sample 45. Two events are missed as g_t does not reach the threshold level. The line of detected events shows transients prior to detection because the time of a jump is obtained from backward calculation.

The higher-order Hinkley detector (H.O.H.D.) works quite similarly: The upward and downward tails in Fig. 3*C* of the test value g_t^8 are smoother than in Fig. 3*B*. Another difference is the successful jump detection at sample 85.

The first-order LOW PASS (Fig. 3*D*) and the eighth-order BESSEL filter (Fig. 3*E*) create a filtered time series which is depicted as a noisy solid line. The subsequent threshold analysis yields the reconstructed time series (solid signal switching between the two levels). The arrows in Fig. 3*D* indicate false alarms of the first-order LOW PASS. There are also missed events. The BESSEL algorithm resolves the same events as the H.O.H.D., but the duration (dwell-time) of the openings is estimated more precisely by the H.O.H.D., as shown by a comparison of the reconstructed signals of Fig. 3*C* and *E* with the ORIGINAL signal in Fig. 3*A*.

This short time series is a simple example because, in our experience, the case with only one channel is seldom found in measured data. Also, the simple model with only one closed state is not realistic. Normally, at least several closed states exist with different lifetimes and sometimes also different open states. Nevertheless, the example of Fig. 3 reveals typical features of the detectors which are essential for discussing which of the detectors is the best for reconstruction of patch-clamp data: the occurrence of false alarms, the missing of brief events, and the reliability of event length estimation. These features are examined in greater detail in the following sections.

Effects of the Selected Time Resolution on the Performance of the Detectors

In a real patch-clamp signal, noise cannot be totally avoided. Therefore, the question arises what time resolution of a detection algorithm can be achieved at a given signal-to-noise ratio.

In order to compare the ability of the detectors to evaluate the correct number and duration of channel openings, a signal with constant open and closed times was analyzed. The adequate signal is a square wave with a closed time of 40 which is long enough to be always detected in the following analysis. The open time of the **periodic** signal is 20 sampling units. The total length was 10,000 samples, thus comprising 166 opening events. The half-jump magnitude p was 0.75 and the white Gaussian noise had a standard deviation σ of 1.0. This signal was analyzed by the four detection algorithms. We varied their time resolution between $t_{res} = 2$ and $t_{res} = 32$ and studied the influence on the resulting open-time histograms (Fig. 4). The resolved open times ought to be equal to 20, the fixed open time of the original square wave. This would result in an ideal open-time histogram with a single bar of height 166 at open time 20.

Column 3 in Fig. 4 shows that the first-order low pass has a significantly higher rate of false alarms (peaks at open time ≈ 1). This is easily understood by an inspection of Fig. 3, showing that the filtered signal tends to cross the threshold three times or more on a falling or rising edge (sample 70 and 230 in Fig. 3) because it is not smooth enough. This is due to the larger amount of high frequencies in the filtered signal as compared with the eight-pole Bessel filter. Therefore, the first-order low pass is excluded from further analysis.

The comparison of columns 4, 2 and 1 for the BESSEL, the H.O.H.D. and the HINKLEY algorithms reveals only slight differences. The false alarms at $t_{res} = 2, 4$ in the upper two rows vanish at longer $t_{res} = 8, 16$. In these two rows, the Hinkley detector and the higher-order Hinkley detector show a smaller error of the estimated open time. In the last row with $t_{res} = 32$, only a few openings are resolved. Most of the openings are missed, because their length of 20 sampling units is significantly shorter than the time resolution.

False Alarms

First, the problem of false alarms is addressed. The adequate method is a simulation with no open event at all. The ORIGINAL signal is constant at the closed level. Nevertheless, the detection algorithm, assuming a jump magnitude $2 \cdot p$, may detect some jumps originating from the noise superimposed on the constant ORIGINAL time series. The signal-to-noise ratio and the time resolution are varied and the number of detected, i.e., "pretended" events is counted. The numbers of false alarms in a time series of one million samples are shown in the boxes

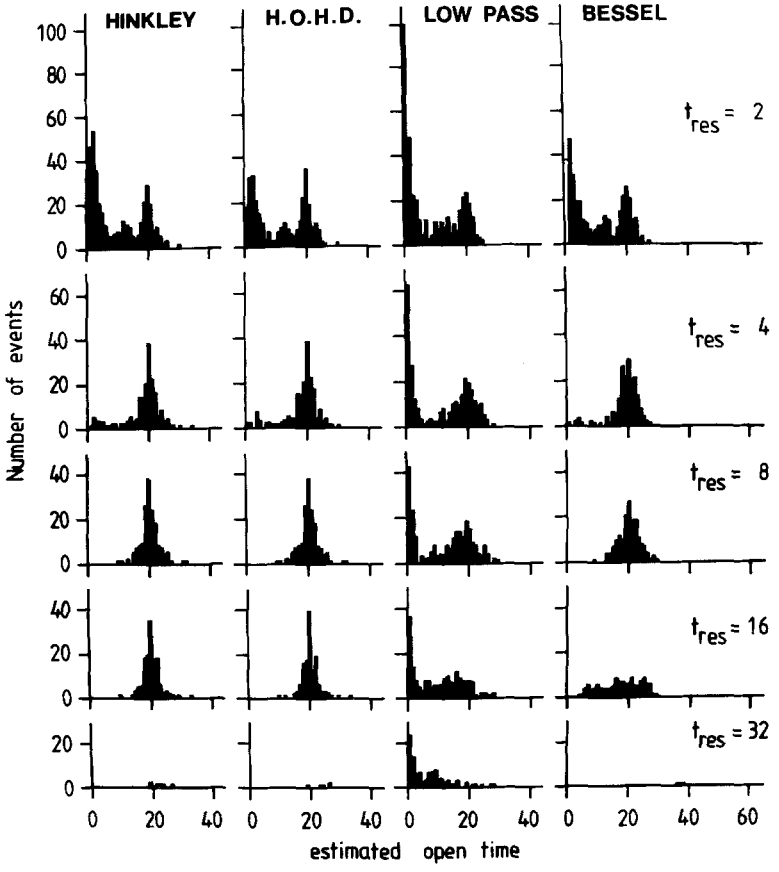

Fig. 4. Open-time histograms from simulated noisy square waves. The signal always has the same parameters: 166 openings of length 20, SNR = 1.5. The histograms are generated by four different detection algorithms. Columns from left to right: HINKLEY, H.O.H.D., LOW PASS, BESSEL. Rows: time resolution changing from 2 at the top to 32 sampling units at the bottom. Notice, that at too short time resolutions all filters show many false events (additional events with open time ≈ 1). This error vanishes for the HINKLEY, H.O.H.D. and BESSEL column at $t_{res} \approx 8$. The bad performance of the LOW-PASS algorithm is obvious. For time resolution 32 which is longer than the opening length (20), the four algorithms miss many events.

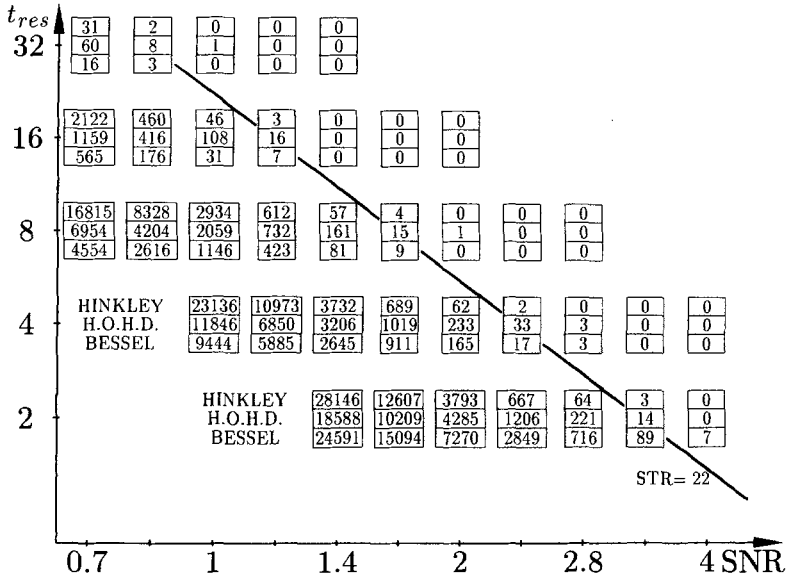

Fig. 5. Number of false alarms from a time series of 1,000,000 points that does not contain any opening at all. The numbers in each box refer (from top to bottom) to the false alarms of the HINKLEY, the H.O.H.D., and the BESSEL detector. The condition for less than 100 false alarms is nearly the same for all detectors: STR > 22 (diagonal line).

of Fig. 5. The SNR axis stands for the quality of the signal. The t_{res} axis describes the sensitivity of the detectors. It is not surprising that the number of false alarms decreases with higher SNR or longer t_{res}. More interesting, however, is the result that all detectors give nearly the same number of false alarms, depending only on the product ($SNR^2 \cdot t_{res}$). Because of the importance of this quantity, we assign a new name to it: "scaled time resolution STR."

$$\mathrm{STR} = \mathrm{SNR}^2 \cdot t_{\mathrm{res}} \tag{12}$$

It roughly stands for the amount of information in a data sequence of length t_{res}, which can be used by a detector for the decision about jumps.

The results for the Hinkley detector are in good agreement with an approximation proposed previously (Schultze, 1992) for the false alarm rate of the Hinkley detector in the presence of white noise:

$$\frac{\text{No. of false alarms}}{1{,}000{,}000} = \exp\left(-\frac{2p\lambda}{\sigma^2}\right) = \exp\left(-\frac{t_{\mathrm{res}} \cdot \mathrm{SNR}^2}{2}\right) \tag{13}$$

The time resolution of the algorithms is set according to the following protocol. Given a time series of pipette current with channel activity, the SNR of the measurement is determined. Then, we have to declare what amount of false alarms we find tolerable. For instance, we have decided to allow 100 false alarms per 1,000,000 sampling steps without any jumps. With this definition in mind, we inspect Fig. 5 and search for the region where the detectors give less than 100 alarms. This leads to the diagonal line in Fig. 5. It divides the t_{res}-SNR plane into two parts. Below the line (STR $<$ 22) more than 100 false alarms occur, above the line (STR $>$ 22) less than 100 false alarms are recorded (within 1,000,000 samples). The rule for the choice of the time resolution in the presence of white noise, therefore, is common for the three detectors

$$t_{\mathrm{res}} = 22/\mathrm{SNR}^2. \tag{14}$$

However, the background noise from the pipette is not white, but rises as f above 1 kHz. In addition, analog filters for antialiasing and noise suppression are used before sampling. All this leads to a colored noise spectrum which probably varies from setup to setup.

The conditions for the following investigation with colored noise are chosen similarly to our experimental setup with a cutoff frequency (−3dB) of our antialiasing Bessel filter set to 25 kHz. This sufficiently suppresses the noise at 50 kHz and higher frequencies. (The sampling frequency f_s is 100 kHz.) The noise spectrum is shown in Fig. 6. We have repeated the above experiment of counting false alarms but have started from a series of one million samples exhibiting our typical patch-clamp spectrum (Fig. 6). Again, the time series contains

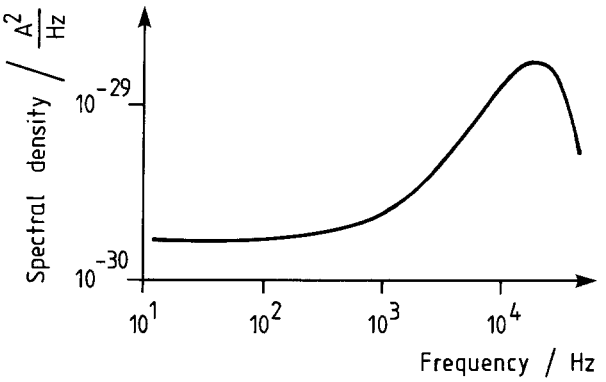

Fig. 6. Noise spectrum of pipette current from our setup. Below 1 kHz, the spectral density is quite flat. Between 1 kHz and 20 kHz it rises as f. Higher frequencies are cut off by the antialiasing Bessel filter.

only the noise, not any opening at all. The results which are listed in Fig. 7 reveal differences between the detectors which no longer allow a general rule like Eq. (14) for the choice of the time resolution. This choice now has to be based directly on the diagram of false alarms (Fig. 7). If, for instance, a time series with SNR = 2.8 is to be analyzed, we find from Fig. 7 that there are no false alarms when t_{res} is chosen 4, 8 or more. At $t_{\mathrm{res}} = 2$ the Bessel filter produces 133 false alarms, the Hinkley detector 50, and the H.O.H.D. only 28. If we tolerate 100 false alarms within 1,000,000 samples, the choice of $t_{\mathrm{res}} = 2$ is okay for the Hinkley detector and the H.O.H.D., but not for the Bessel filter.

Since one is normally interested in the shortest possible time resolution, the H.O.H.D. is the preferable method for this example with SNR = 2.8.

If, however, the measured time series had a worse SNR of about 1.0, the achievable time resolution would be about eight sampling steps and the lowest rate of false alarms would be produced by the Bessel algorithm. With this kind of noisy measurements, fast processes on a time scale of about two or three sampling steps could not be investigated with any detection algorithm.

The dependence of the achievable time resolution on the specific noise spectrum makes it impossible to present general numerical results. If the reader wants to find out the possible time resolution of his/her patch-clamp setup, we therefore recommend saving a time series without channel activity and performing an experiment of counting false alarms as described above. A diagram like that in Fig. 7 can be constructed from a single, noisy time series without any channel opening. These results supply a basis for the choice of the time resolution, depending on the signal-to-noise ratio.

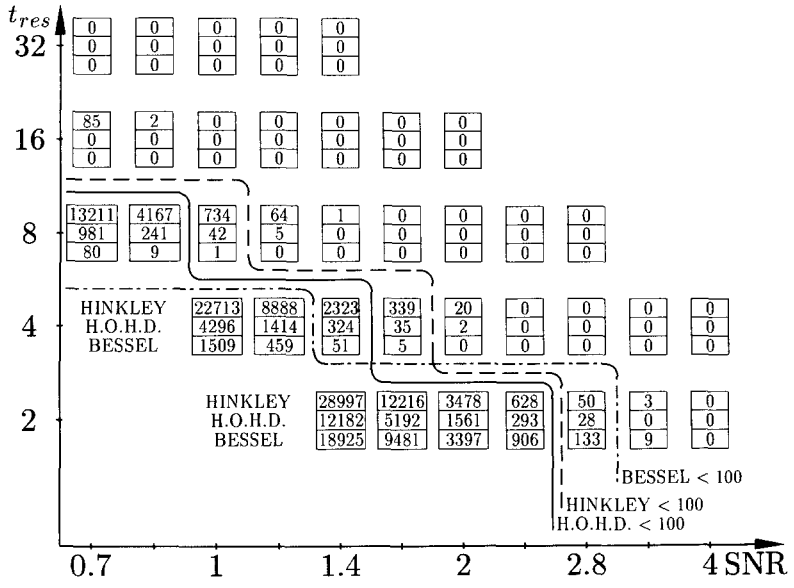

Fig. 7. Number of false alarms from a colored noise series of one million samples without any opening at all. In contrast to Fig. 5 we have used colored noise (*see* Fig. 6). The numbers in each box refer (from top to bottom) to the false alarms of the HINKLEY, the H.O.H.D., and the BESSEL detector. The condition for less than 100 false alarms (indicated by the solid and dashed lines) is no longer the same for the three detectors.

Missed Events

The problem of missing short events is already mentioned when describing Figs. 3 and 4. Again, we use **periodic** square wave signals with long closed times and short openings. The time resolution of the detectors is kept constant at $t_{res} = 12$. The closed time of 40 sampling steps is long enough to be always detected, i.e., no closure is missed. The open time is varied between 4 and 24 sampling steps. Thus, the openings are short enough to be partially missed by the detector. The percentage of detected openings is plotted *vs.* the real open time in Fig. 8. In the absence of noise, the step function (broken line) holds because all events longer than $t_{res} = 12$ are detected, all shorter events are not. In the presence of white noise with SNR = 1.41 some events longer than t_{res} are missed if the noise makes the event look shorter or flatter. On the other hand, shorter events than t_{res} may be enhanced by the noise. These effects result in the soft transitions shown in Fig. 8. Compared with the HINKLEY technique the higher-order BESSEL and H.O.H.D. algorithms offer a sharper cutoff at the specified time resolution.

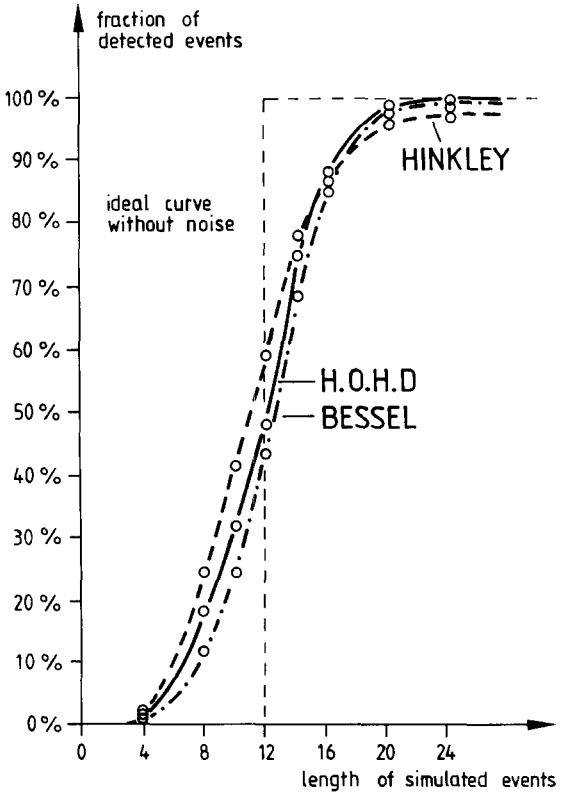

Fig. 8. Fraction of detected events *vs.* the event length. The signal-to-noise ratio is SNR = 1.41, and the time resolution of all three detectors is $t_{res} = 12$ sampling units. In the presence of a noise-free signal all events shorter than t_{res} would be missed and all events longer than t_{res} would be detected, thus giving the step function (broken line) as the ideal result.

Estimation of Event Length

We use square-wave signals like those for Fig. 4 and study the influence of the signal-to-noise ratio SNR and the time resolution t_{res} on the accuracy of the open-time estimation. We take the standard deviation of the difference between the estimated open times and the correct open time as "estimation error." This standard deviation is easily obtained from the open-time histograms similar to those in Fig. 4. The results are depicted in Fig. 9 which shows the dependence of the estimation error on the signal-to-noise ratio. As already mentioned

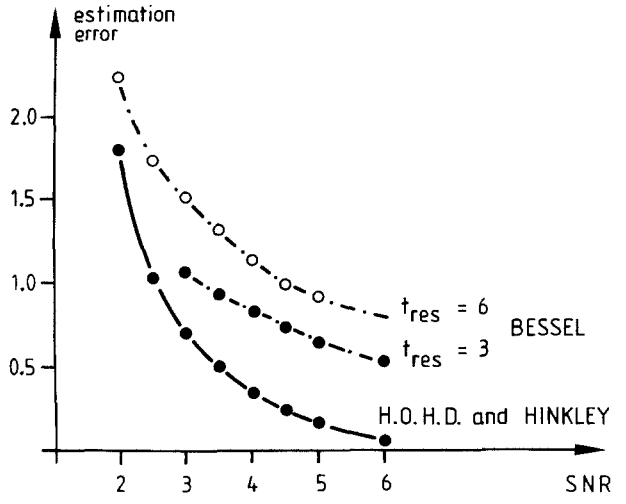

Fig. 9. Standard deviation of open-time estimation error for long openings (compared with the time resolution) depending on the signal-to-noise ratio. The time resolution of the detectors is 3 or 6. The HINKLEY and the H.O.H.D. algorithms offer the same accuracy, independent of time resolution, because the estimated jump time does not depend on the time when the jump is detected.

(Fig. 4) the accuracy of the estimated open time is better in the case of the nonlinear Hinkley and H.O.H.D. detectors than with the Bessel filter. Even worse is the peculiar dependence of the Bessel error (dash-dot-lines in Fig. 9) on the time resolution. With longer t_{res}, which may be thought to be an "easier task" for the Bessel detector, the estimation error increases. This deteriorates the apparently good performance (Fig. 7) of the Bessel algorithm at long t_{res}, because the low rate of false alarms is accompanied with a bad estimation of event length.

So far, we have evaluated the estimated dwell-time of an opening, irrespective to a temporal shift of the whole opening event. In experiments with channels activated by external stimuli the jump time itself may be of interest. In this case, the deterministic delay of the Bessel filter (*compare* the reconstructed signal in Fig. 3*E* with the ORIGINAL signal in Fig. 3*A*) becomes important and the results have to be corrected for this delay. The jump time estimation of the Hinkley detector and the H.O.H.D. is more exact and does not include a deterministic delay. The superiority of the Hinkley detector and the H.O.H.D. is due to the separation between jump detection (influenced by t_{res}) and estimation of the jump moment (independent of t_{res}).

In order to study the estimation of event length with more than one channel under investigation, we have simulated two identical channels with one closed and one open state as shown in Eq. (11) and rate constants $k_{oc} = 0.05$, $k_{co} = 0.03$ as used for Fig. 3. The signal-to-noise ratio (white noise) is SNR = 3 and the time resolution is $t_{res} = 3$. This example is quite simple but nevertheless shows a typical error of the Bessel algorithm when more than one channel, i.e., more than two levels are involved.

The evaluation of the simulated data results in three dwell-time histograms (one for each level 0, 1, 2) for each of the three detectors (BESSEL, HINKLEY, H.O.H.D.). All these nine dwell-time histograms start at bin $t = 1$ with an upward slope because of missed events. The maximum is found near the time resolution t_{res} in the bins $t = 3$ or $t = 4$. The downward slope $t > 6$ is not affected by missed events. This range may be used for reliable exponential fits. In the histograms for the intermediate level 1, however, the BESSEL filter creates an additional peak at the maximum of the histogram. This peak may lead to the misinterpretation that an additional, fast time constant is involved. Our simulations have shown that this effect arises from the following artifact: When two channels open (or close) nearly simultaneously the dwell-time in the intermediate level is very short, but the Bessel-filtered signal rises (or decays) somewhat slower than the original signal and stays longer in the interval related to level 1. This leads to an overestimation of short dwell-times of intermediate levels. The Hinkley detector and the H.O.H.D. do not have any difficulties because the two subsequent jump times are estimated by backward calculation, independent of the procedure of jump detection.

Results from Real Data

We applied the Hinkley, H.O.H.D. and Bessel algorithms to a record over 60 seconds from a droplet of *Chara corallina,* prepared as described in a previous paper (Draber et al., 1991). The experimental solution contained 250 mM KCl and 5 mM $CaCl_2$. The current signal was sampled and AD-converted at 100 kHz. The time series contained 6,000,000 sampled current values. At a voltage of $V = 50$ mV the single channel current was 9 pA, the standard deviation of noise was $\sigma = 2.2$ pA, resulting in a SNR of 4.1. Figure 1*A* shows an 80-msec part (8,000 samples) of the data.

Dwell-time histograms for each level of pipette current were produced by the three different detectors. At dwell-times longer than 0.4 msec (40 sampling units) the three detection algorithms gave the same results, but there were also a lot of short events in the time series (Fig. 1*A*). The H.O.H.D. detected the highest amount of them. Figure 1*B* shows the H.O.H.D.-based dwell-time histogram of

the closed level (all channels closed). The fit of two exponentials yielded a fast time constant of 48 μsec which was, until now, beyond the time resolution of patch-clamp event detection. Results and adequate models will be presented in a subsequent paper.

Discussion

The detection algorithm for patch-clamp data has to provide the following features:

(i) No waste of information: The time resolution has to be as short as possible under the constriction that no false alarms occur. In the presence of white noise the HINKLEY, H.O.H.D. and BESSEL algorithms offer the same quality (Fig. 5). In real experiments the noise is not white. In this situation the H.O.H.D. algorithm shows the best performance at high temporal resolution (Fig. 7).

(ii) Sharp cutoff at given time resolution: For theoretical considerations (Blatz & Magleby, 1986; Crouzy & Sigworth 1990) of missed brief events, it is necessary that nearly all events longer than the selected time resolution are detected and all shorter events are not. With regard to this aspect, the H.O.H.D. and the BESSEL detection algorithms are superior to the HINKLEY detector (Fig. 8).

(iii) Exact estimation of event duration: An unreliable estimation of event length leads to a distortion of the dwell-time histograms. The Hinkley and the H.O.H.D. detectors estimate the event duration of detected events with the same algorithm, looking for minima and maxima of the cumulative sum. The results do not depend on the selected time resolution and are very precise compared with the BESSEL algorithm looking for threshold crossings. The determination of the event length by means of the Bessel filter is especially bad when a long time resolution is used (Fig. 9).

These arguments lead to the conclusion that the H.O.H.D. is the best algorithm for reconstruction of patch-clamp data.

In addition to the advantages presented of the nonlinear off-line H.O.H.D. algorithm over the linear off-line BESSEL filter, we want to emphasize the general superiority of off-line analysis. Most workers use analog Bessel filters whose time resolution has to be set a priori without knowing the signal-to-noise ratio of the later experiment. The knowledge of SNR is required for the optimal setting of t_{res} (setting of cutoff frequency). Moreover, when using different command voltages with one patch the signal-to-noise ratio changes during the experiment, and it is practically impossible to set the filter cutoff exactly to the edge of a tolerable false alarm rate.

Therefore, we strongly recommend off-line analysis, preferably by means of the higher-order Hinkley detector, using an analog Bessel filter only for antialiasing.

The program used here was written in Turbo Pascal (program listings available on request). On an 80386 personal computer with 20 MHz it takes about nine minutes to apply the H.O.H.D. to a time series of one million samples, depending slightly on the number of channels within the patch.

This work emerged from a research project at Anschütz & Co., Kiel, Germany, concerned with the detection of parameter jumps in a dynamic system, which is realized in cooperation with the Biophysics and System Identification Group at Kiel University (Prof. Dr. U.-P. Hansen). We gratefully acknowledge the financial support and the computer capacities from Anschütz & Co. The experimental investigations were supported by the Deutsche Forschungsgemeinschaft (Ha 712/7-5). We are very grateful to Prof. Dr. Ulf-Peter Hansen who made this work possible and accompanied it with helpful and critical discussions. The 100 kHz data acquisition setup, including the tunable Bessel filter, was built by Dipl.-Phys. Arne Albertsen. We thank Prof. Dr. Thomas Holzhüter for hints to literature and for initiating the cooperation between university and industry. Dipl.-Phys. Christian Ruge made valuable suggestions increasing the readability of the manuscript. We are grateful to Mrs. E. Götting for drawing many of the figures.

References

Antoniou, A. 1979. Digital Filters: Analysis and Design. pp. 129–130, 168–171. McGraw-Hill, New York

Basseville, M. 1986. Detection of changes in signals and systems. *In:* Preprints of 2nd IFAC Workshop on Adaptive Systems in Control and Signal Processing, 1.-3.7.1986, Lund Institute of Technology. K.J. Åström and B. Wittenmark, editors. pp. 7–12

Basseville, M., Benveniste, A., eds. 1986. Detection of Abrupt Changes in Signals and Dynamical Systems. Springer-Verlag, Berlin, Heidelberg, New York, Tokyo

Bertl, A. 1989. Current-voltage relationships of a sodium-sensitive potassium channel in the tonoplast of *Chara corallina*. *J. Membrane Biol.* **109:**9–19

Blatz, A.L., Magleby, K.L. 1986. Correcting single channel data for missed events. *Biophys. J.* **49:**967–980

Colquhoun, D., Sigworth, F.J. 1983. Fitting and statistical analysis of single channel records. *In:* Single-Channel Recording. B. Sakmann and E. Neher, editors. pp. 191–263. Plenum, New York, London

Crouzy, S.C., Sigworth, F.J. 1990. Yet another approach to the dwell-time omission problem of single-channel analysis. *Biophys. J.* **58:**731–743

Draber, S., Schultze, R., Hansen, U.-P. 1991. Patch-clamp studies on the anomalous mole fraction effect of the K^+-channel in cytoplasmic droplets of *Nitella:* an attempt to distinguish between a multi-ion single-file pore and an enzyme kinetic model with lazy state. *J. Membrane Biol.* **123:**183–190

FitzHugh, R. 1983. Statistical properties of the asymmetric random telegraph signal with application to single-channel analysis. *Math. Biosci.* **64:**75–89

Hedrich, R., Schroeder, J.I. 1989. The physiology of ion channels and electrogenic pumps in higher plants. *Annu. Rev. Plant. Physiol.* **40:**539–569

Heinemann, S.H., Sigworth, F.J. 1988. Open channel noise. IV. Estimation of rapid kinetics of formamide block in gramicidin A channels. *Biophys. J.* **54:**757–764

Hinkley, D.V. 1971. Inference about the change-point from cumulative-sum tests. *Biometrika* **57:**1–17

Klieber, H.-G. 1990. Kinetik von Ionenkanälen aus *Chara corallina*. Ph.D. thesis Universität Göttingen

Nikiforov, I.V. 1986. Sequential detection of changes in stochastic systems. *In:* Preprints of 2nd IFAC Workshop on Adaptive Systems in Control and Signal Processing, 1.-3.7.1986, Lund Institute of Technology. K.J. Åström and B. Wittenmark, editors pp. 167–173

Page, E.S. 1954. Continuous inspection schemes. *Biometrika* **41:**100–115

Page, E.S. 1955. A test for a change in parameter occurring at an unknown point. *Biometrika* **42:**523–527

Pietrobon, D., Prod'hom, B., Hess, P. 1988. Conformational changes associated with ion permeation in L-type calcium channels. *Nature* **333:**373–376

Sakmann, B., Neher, E. eds. 1983. Single-Channel Recording. Plenum, New York, London

Schultze, R. 1992. Robust identification for adaptive control: the dynamic Hinkley-detector. *In:* Preprints of ACASP'92, IFAC Symposium on Adaptive Systems in Control and Signal Processing, 1-3.7.1992. Grenoble, France

Yellen, G. 1984. Ionic permeation and blockade in Ca^{2+}-activated K^+ channels of bovine chromaffin cells. *J. Gen. Physiol.* **84:**157–186

Received 28 January 1992; revised 20 July 1992